Line Shape Distortion in a Nonlinear Auto-Oscillator Near Generation Threshold: Application to Spin-Torque Nano-Oscillators

Joo-Von Kim,* Q. Mistral, and C. Chappert

Institut d'Electronique Fondamentale, UMR CNRS 8622, Université Paris-Sud, 91405 Orsay, France

V. S. Tiberkevich and A. N. Slavin

Department of Physics, Oakland University, Rochester, Michigan 48309, USA

(Received 29 September 2007; published 22 April 2008)

The power spectrum of an auto-oscillator with a large frequency nonlinearity in a noisy environment is calculated. The power spectrum becomes strongly non-Lorentzian, broadened, and asymmetric near the generation threshold. A Lorentzian spectrum is recovered far below and far above the threshold, which suggests that line shape distortions provide a signature of the threshold. We show that the developed theory adequately describes the observed behavior of a strongly nonlinear spin-torque nano-oscillator.

DOI: 10.1103/PhysRevLett.100.167201 PACS numbers: 85.75.−d, 05.10.Gg, 75.30.Ds, 75.40.Gb

Thermal noise plays a key role in the dynamics of auto-oscillatory systems, especially for the nanosized systems in which the characteristic oscillation energy is comparable with the thermal noise energy $k_B T$. One important effect of noise is spectral line broadening. It is well established, for example, that a broadened Lorentzian power spectrum results from white Gaussian noise in conventional auto-oscillators (for which the frequency is weakly dependent on the amplitude), in the regimes both far below and far above the auto-oscillation threshold [1,2]. In the immediate vicinity of the threshold, the power spectrum is non-Lorentzian but can be described by a sum of partial Lorentzians with the same central frequency [2]. Such higher-order terms are small in a conventional auto-oscillator and do not lead to any significant changes to the shape of the power spectrum. In a *nonlinear* auto-oscillator, on the other hand, the central frequencies of the partial Lorentzian profiles are frequency shifted by different amounts due to the strong dependence of the amplitude on frequency. In this Letter, we show that such nonlinearities lead to a significant broadening and asymmetry of the spectral line near threshold.

An example of an auto-oscillator with strong frequency nonlinearity is the spin-transfer nano-oscillator (STNO). The STNO consists of two (“free” and “fixed”) ferromagnetic layers separated by a nonmagnetic (metallic or dielectric) spacer. Because of the spin-transfer effect [3,4], the passage of a spin-polarized current through the multilayer leads to an effective negative damping in the free layer. The induced negative damping overcomes the natural positive damping if the current is sufficiently large, and auto-oscillations of magnetization in the free layer are excited [5–7]. These and related phenomena are subjects of intensive research at present due to their possible applications in microwave nanoelectronics.

In this Letter, we present a theory of line shape distortion in auto-oscillators with a strong nonlinear frequency shift in the presence of thermal noise. We show that line broadening and line asymmetry are key signatures of the threshold region, and we argue that such features provide a direct means of determining the threshold in experiment. This point is especially significant for STNOs in which the influence of noise on the device performance is of a qualitative importance. Good qualitative agreement is found with recent experiments on STNO nanopillars.

Our theory is based on a spin-wave Hamiltonian formalism for magnetic multilayers with spin transfer [8,9]. We assume only *one* spin-wave mode—the mode with the lowest relaxation rate—is excited at the auto-oscillation threshold. This mode dominates the dynamics both below and just above threshold. With this assumption we reduce the Landau-Lifshitz equation with Gilbert damping, which describes the magnetization dynamics of the STNO free layer, to a stochastic oscillator equation for the complex amplitude c of the excited mode ($|c| \le 1$) [8,10,11],

$$\frac{dc}{dt} + i\omega(p)c + \Gamma_+(p)c - \Gamma_-(I, p)c = f(t). \tag{1}$$

Here, $p = |c|^2$ is the dimensionless oscillation power which determines the polar angle θ of the magnetization precession in the free layer $\theta \equiv \arccos(M_z/M_0) = \arccos(1 - 2|c|^2)$, where M_0 is the length of the magnetization vector and M_z is the projection of this vector on the direction of stationary equilibrium magnetization $\mathbf{z}$ [8]. The oscillation frequency is $\omega(p) \simeq \omega_0 + Np$, where ω_0 is the (linear) mode frequency, and the coefficient N describes a nonlinear frequency shift. Typically for STNOs, $|N| \gtrsim \omega_0$, which is the distinguishing feature from other conventional “quasilinear” auto-oscillators for which $N \simeq 0$. The second term in Eq. (1), $\Gamma_+(p) \simeq \Gamma_0(1 + Qp)$, represents natural *positive* spin-wave damping, where Γ_0 is the linear relaxation rate and Q is the phenomenological dimensionless parameter characterizing nonlinearity of the damping [12]. The third term, $\Gamma_-(I, p) = \sigma I(1 - p)$, describes current-induced nonlinear damping (which is *negative* for small oscillation amplitudes), where I is the bias current and σ is the spin-polarization efficiency defined by Eq. (5) in Ref. [8]. We stress that the nonlinear oscillator equation (1) is general; it applies not only to spin-transfer-induced dynamics in magnetic multilayers, but also to the dynamics of *any* nonlinear auto-oscillating system operating in a single-mode regime.

The function $f(t)$ in (1) is stochastic and describes the influence of fluctuations. We take $f(t)$ to be a white Gaussian process with zero mean and spectral properties $\langle f(t)f^*(t')\rangle = 2\Gamma_0\eta\delta(t-t')$. The amplitude of fluctuations is governed by the relaxation frequency Γ_0 of the free layer and the thermal noise energy $\eta = k_BT/(\lambda\omega_0)$, where λ relates the oscillation power to the system energy $E(p) = \lambda\omega_0 p$. For STNOs $\lambda = VM_0/\gamma$, where V is the volume of magnetic material involved in auto-oscillations and γ is the gyromagnetic ratio. This choice of η ensures that the system, in the absence of spin transfer, relaxes towards the equilibrium thermal noise level $\langle E(c)\rangle = k_BT$ at the rate Γ_0 [10,11]. The statistical properties of $f(t)$ are consistent with the linear expansion of the exact stochastic force in the Landau-Lifshitz equation with random thermal fields. Higher-order terms [of the form $f'(t)c$] are negligible near the generation threshold since $|c| \ll 1$.

In STNO experiments the magnetization oscillations are characterized by the spectral density of voltage oscillations $v(t)$ arising from magnetoresistance variations. The autocorrelation function of $v(t)$ is directly proportional to the autocorrelation function of the corresponding spin-wave oscillations to lowest order [10], i.e., $\langle v(t)v(0)\rangle \propto \mathrm{Re}[\langle c(t)c^*(0)\rangle]$. In what follows, we show how to obtain the correlation function $K(t) \equiv \langle c(t)c^*(0)\rangle$ or the power spectrum,

$$S(\omega) \equiv \int_{-\infty}^{\infty} K(t)e^{i\omega t}dt, \qquad (2)$$

of spin-wave oscillations described by (1) for any magnitude of the bias current.

The spin-wave correlation function can be evaluated exactly in limiting cases. In the subcritical regime, $\zeta \equiv I/I_{\rm th} \ll 1$ (where $I_{\rm th} \equiv \Gamma_0/\sigma$ is the threshold current at which the auto-oscillations start), all nonlinearities can be ignored and Eq. (1) leads to a Lorentzian power spectrum $S(\omega)$ with linewidth

$$\Delta\omega = \Gamma_0 - \sigma I. \qquad (3)$$

This linear dependence has been observed in spin-valve nanopillars [13] and tunnel junctions [14] at low bias. Far above threshold ($\zeta > 1$), the line shape is also Lorentzian with a linewidth governed by phase noise [10,15],

$$\Delta\omega = \Gamma_0(k_BT/E_0)[1 + (N/\Gamma_{\rm eff})^2], \qquad (4)$$

where $E_0 = \lambda\omega_0 p = \lambda\omega_0(\zeta-1)/(\zeta+Q)$ is the average energy of the stable auto-oscillation in STNO, $N = d\omega(p)/dp$, and $\Gamma_{\rm eff} = d\Gamma_+(p)/dp - d\Gamma_-(p)/dp$ is the effective nonlinear damping (see Ref. [15] for details).

Near threshold, the coupling between amplitude and phase fluctuations leads to a non-Lorentzian power spectrum. To see this, let $c(t) = r(t)\exp[i\phi(t) - i\omega_0 t]$ and linearize (1) about the steady-state trajectory, $r_0 = \sqrt{(\zeta-1)/(\zeta+Q)}$, just above threshold, $r(t) = r_0 + a(t)$ [15]. We find $\dot a(t) + 2\Gamma_{\rm eff}r_0^2 a(t) = \mathrm{Re}[\tilde f(t)]$ and $\dot\phi(t) = r_0^{-1}\mathrm{Im}[\tilde f(t)] - 2Nr_0 a(t)$. $\tilde f(t) = f(t)e^{i\omega_0 t - i\phi(t)}$ is a white Gaussian noise with the same statistical properties as $f(t)$. While the amplitude fluctuations $a(t)$ are subjected to a white-noise forcing only, $a(t)$ itself becomes a colored-noise source for the phase fluctuations $\phi(t)$, since $\langle a(t)a(t')\rangle \sim \exp(-2\Gamma_{\rm eff}r_0^2|t-t'|)$. The phase variable $\phi(t)$ is therefore driven by a colored-noise source $a(t)$ and a white-noise source $\tilde f(t)$, which leads directly to a non-Lorentzian power spectrum for the phase fluctuations.

This linearization scheme is not accurate in the threshold region, however, because the steady-state amplitude r_0 is comparable to the magnitude of amplitude fluctuations. Instead of solving the full *nonlinear* stochastic problem (1), it is more tractable to solve the corresponding *linear* Fokker-Planck equation, which describes the time evolution of the probability density function (PDF) $\mathcal{P}(t, c; c_0)$. A similar approach has been used to study thermally assisted magnetization reversal with spin-transfer [16] and telegraph noise in bistable current-induced precessional states [17]. The PDF $\mathcal{P}(t, c; c_0)$ gives the probability of having an amplitude c at time t, given the initial amplitude c_0 at $t = 0$. From this nonstationary PDF $\mathcal{P}(t, c; c_0)$, the correlation function $K(t)$ for $t > 0$ can be obtained as

$$K(t) = \int d^2c \int d^2c_0 \mathcal{P}(t, c; c_0)\mathcal{P}_0(c_0)cc_0^*, \qquad (5)$$

where $\mathcal{P}_0(c)$ is the stationary PDF, i.e., $\mathcal{P}_0(c) = \lim_{t\to\infty}P(t, c; c_0)$. For $t < 0$ one can use relation $K(t) = K^*(-t)$.

The linear Fokker-Planck equation can be obtained from (1) in a standard way [18], which in polar coordinates is given by

$$\frac{\partial\mathcal{P}}{\partial t} = \frac{1}{r}\frac{\partial}{\partial r}\{[\Gamma_+(r^2) - \Gamma_-(I, r^2)]r^2\mathcal{P}\} + Nr^2\frac{\partial\mathcal{P}}{\partial\phi} + \eta\Gamma_0\left[\frac{1}{r}\frac{\partial}{\partial r}\left(r\frac{\partial\mathcal{P}}{\partial r}\right) + \frac{1}{r^2}\frac{\partial^2\mathcal{P}}{\partial\phi^2}\right] \equiv \hat L\mathcal{P}. \qquad (6)$$

The stationary solution $\mathcal{P}_0$ of Eq. (6) does not depend on the time t and angle ϕ, i.e., $\mathcal{P}_0 = \mathcal{P}_0(r)$, and can be found explicitly in a general case [11]. Equation (6) is a linear equation that does not depend on time t and phase ϕ explicitly. Therefore, its solution $\mathcal{P}(t, c; c_0) = \mathcal{P}(t, r, \phi; r_0, \phi_0)$ can be written as a series

$$\mathcal{P}(t, r, \phi; r_0, \phi_0) = \sum_{n,\mu} a_{n,\mu}(r_0, \phi_0) P_{n,\mu}(r) e^{-\Lambda_{n,\mu} t - in\phi}, \tag{7}$$

where $P_{n,\mu}(r)$ are normalized eigensolutions of the problem $\hat{L}_n P_{n,\mu} = -\Lambda_{n,\mu} P_{n,\mu}$, with $\hat{L}_n \equiv \hat{L}(\partial_r, -in)$. The eigenvalues $\Lambda_{n,\mu}$ and coefficients $a_{n,\mu}(r_0, \phi_0)$ satisfy the initial conditions for the PDF: $\mathcal{P}(0, r, \phi; r_0, \phi_0) = (1/r)\delta(r - r_0)\delta(\phi - \phi_0)$. In the expansion (7), the index n describes the ϕ dependence $\sim \exp(-in\phi)$ of the particular statistical mode $P_{n,\mu}$, while the index μ enumerates different modes having the same ϕ dependence.

With the normalized solutions $Q_{n,\mu}(r)$ of the adjoint eigenproblem, $\hat{L}_n^+ Q_{n,\mu} = -\Lambda_{n,\mu}^* Q_{n,\mu}$, and using (5) and (7) with (2), we obtain a series expansion for the power spectrum $S(\omega)$,

$$S(\omega) = \sum_{\mu} \frac{F_{1,\mu} \operatorname{Re}(\Lambda_{1,\mu})}{[\omega - \operatorname{Im}(\Lambda_{1,\mu})]^2 + [\operatorname{Re}(\Lambda_{1,\mu})]^2}, \tag{8}$$

whereby each contribution is weighted by the factor $F_{1,\mu} = \int_0^\infty dr \int_0^\infty dr' (rr') P_{1,\mu}(r) \mathcal{P}_0(r) Q_{1,\mu}^*(r')$. Each term in (8) is associated with one statistical eigenmode (n, μ). Only the $n = 1$ modes give contributions to the second-order correlator $K(t)$ and power spectrum $S(\omega)$; modes with other phase indices n are needed to calculate higher-order correlators, such as $\langle [c^*(t)c(0)]^2 \rangle$. The line shape associated with each mode is Lorentzian, with the central frequency and linewidth given by the imaginary and real parts of the eigenvalues $\Lambda_{1,\mu}$, respectively. The result in (8), therefore, represents an expansion of the power spectrum in terms of partial Lorentzians, whereby each mode describes an additional relaxation process due to colored-noise sources.

Line shape asymmetry is important only when several statistical modes have comparable partial linewidths $\operatorname{Re}(\Lambda_{1,\mu})$ and/or weight factors $F_{1,\mu}$. This situation occurs in the region just above the generation threshold, which is illustrated in Fig. 1. The noise level considered is $\eta = 10^{-3}$, which is approximately equivalent to $T = 300$ K for the nanopillar system in [19] and $T = 400$ K for the nanocontact system in [7] with an in-plane applied field of 0.6 T. Far below and above threshold, the spectral lines are largely Lorentzian and are well described by a single $\mu = 1$ mode for which the weighting factor $F_{1,1}$ is at least 2 orders of magnitude larger than the others, as one can clearly see in Fig. 1. A significant deformation of the spectral line occurs near and just above threshold, as discussed earlier, which appears as large contributions from the higher-order eigenmodes in (8). For the nonlinear oscillator, there is an additional line shape asymmetry due to the different central frequencies of the partial Lorentzians. As each term represents a different amplitude process, the associated frequency shift is also different for each term.

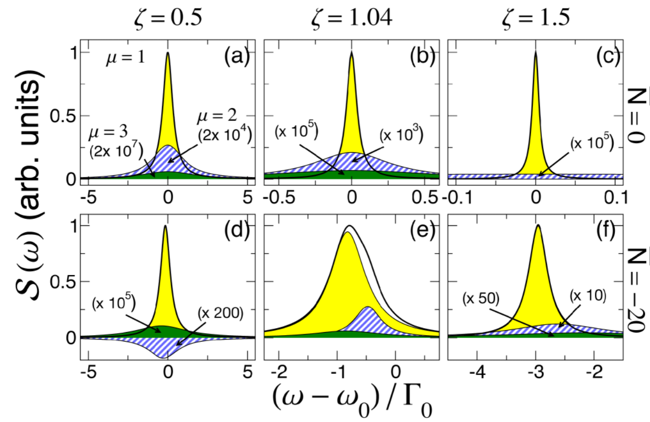

FIG. 1 (color online). Power spectrum, $\mathcal{S}(\omega)$, for $\eta = 10^{-3}$ and $Q = 2$. The dominant μ modes contributing to the overall spectral line (thick black curve) are shown for two values of frequency nonlinearity $\bar{N} = N/\Gamma_0$ at different supercriticality $\zeta = I/I_{\mathrm{th}}$.

Salient features of this line shape asymmetry have been observed in a recent experiment [19]. In Fig. 2, the experimental spectral lines are fitted and compared with the theoretical line shapes predicted by Eq. (8). Based on the experimental linewidth and power variations we estimated the experimental critical current to be $I_c = 5.2$ mA, which allows us to compare the theoretical and experimental line shapes at the same supercriticality ζ. Below threshold ($I = 5.0$ mA, $\zeta \approx 0.96$) the experimental data are well described by a single Lorentzian curve [Fig. 2(e)], which is consistent with the theoretical curve [Fig. 2(a)]. Just above threshold ($I = 5.4$ mA, $\zeta \approx 1.04$), a slight asymmetry appears in the spectral line whereby a second Lorentzian peak is required for a reasonable fit. The presence of a second mode is also seen in the theoretical curve, with a

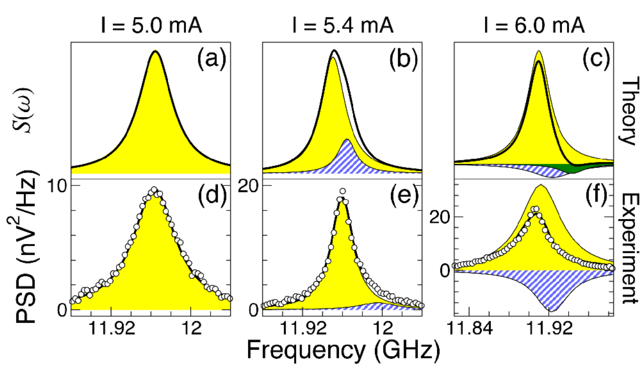

FIG. 2 (color online). Comparison of theoretical and experimental power spectral density (PSD) near threshold ($I_{\mathrm{th}} = 5.2$ mA). Thick solid lines in (a)–(c) represent spectral lines as predicted by Eq. (7), with the first dominant μ modes shown as shaded curves. Circles in (d)–(f) are experimental data at $T = 225$ K taken from Ref. [19], with thick solid lines representing a double Lorentzian fit. Shaded curves are individual Lorentzian profiles used in the fits.

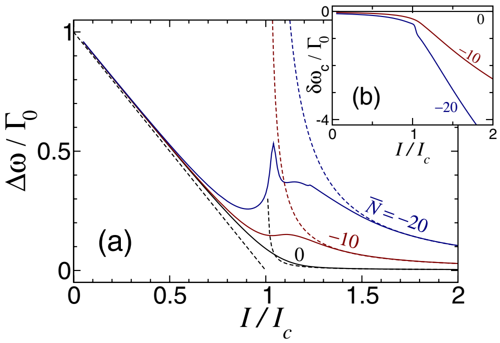

FIG. 3 (color online). (a) Scaled linewidth and (b) frequency shift, $\delta\omega_c = \omega_c - \omega_0$, as a function of supercriticality from Lorentizian fits to spectra computed for different $\bar{N} = N/\Gamma_0$ for $Q = 2$, $\eta_0 = 10^{-3}$. Dashed lines in (a) correspond to Eqs. (3) and (4).

good qualitative agreement in the relative positions and amplitudes of the two modes [Fig. 2(b)]. At a moderate above-threshold current ($I = 6.0$ mA, $\zeta \approx 1.15$), the line shape distortion becomes more pronounced [Fig. 2(f)], and this asymmetry is qualitatively reproduced by the theory [Fig. 2(c)].

Another way to quantify line shape distortion is to fit the spectra with single Lorentzian profiles, which yields a single central frequency ω_c and linewidth $\Delta\omega$. The results of fits of the peaks computed from Eq. (7) for different nonlinearities are shown in Fig. 3. We find good agreement between the numerically and analytically calculated linewidths far below and far above the threshold in all cases, as indicated by the dashed lines representing Eqs. (3) and (4), respectively. In general, the overall linewidth $\Delta\omega$ decreases with increasing current [Fig. 3(a)], except in the region near the generation threshold in which a local linewidth maximum appears because of line shape asymmetry. This maximum can be several times larger than the linewidth in both the subcritical and supercritical regimes, depending on the magnitude of N. Experimental measurements of power spectral variations with bias current [19] are consistent with our theory, which predicts line narrowing followed by line broadening near the threshold (see Fig. 3c of Ref. [19]). The measured current dependence of the oscillation frequency (see Fig. 3a in [19]) is also consistent with our predictions, whereby a weak dependence is seen below threshold followed by a fast quasi-linear decrease above threshold [Fig. 3(b)]. It would be interesting to verify experimentally the predicted linewidth and frequency variations as a function of the nonlinearity N, which could be achieved by examining the power spectrum at different magnetization angles [8,15]. Only frequency redshifts ($N < 0$) have been presented here for the sake of brevity; similar behavior, but with increasing frequency, is predicted for $N > 0$.

In summary, we have presented a theory of line shape distortion for auto-oscillators with strong frequency nonlinearities. The power spectrum becomes asymmetric in the threshold region. Good qualitative agreement with recent experimental data on the spin-transfer nano-oscillators is demonstrated.

This work was in part supported by MURI Grant No. W911NF-04-1-0247 from the U.S. Army Research Office, Contract No. W56HZV-07-P-L612 from the U.S. Army TARDEC, RDECOM, Grant No. ECCS-0653901 from the National Science Foundation of the U.S.A., the Oakland University Foundation, and the European Communities program IST under Contract No. IST-016939 TUNAMOS.

*joo-von.kim@u-psud.fr

[1] A. Blaquiere, *Nonlinear System Analysis* (Academic, New York, 1966).
[2] R. D. Hempstead and M. Lax, Phys. Rev. **161**, 350 (1967).
[3] J. C. Slonczewski, J. Magn. Magn. Mater. **159**, L1 (1996).
[4] L. Berger, Phys. Rev. B **54**, 9353 (1996).
[5] M. Tsoi *et al.*, Phys. Rev. Lett. **80**, 4281 (1998).
[6] S. I. Kiselev *et al.*, Nature (London) **425**, 380 (2003).
[7] W. H. Rippard *et al.*, Phys. Rev. Lett. **92**, 027201 (2004).
[8] A. N. Slavin and P. Kabos, IEEE Trans. Magn. **41**, 1264 (2005).
[9] S. M. Rezende *et al.*, Phys. Rev. Lett. **94**, 037202 (2005).
[10] J.-V. Kim, Phys. Rev. B **73**, 174412 (2006).
[11] V. Tiberkevich, A. Slavin, and J.-V. Kim, Appl. Phys. Lett. **91**, 192506 (2007).
[12] V. Tiberkevich and A. Slavin, Phys. Rev. B **75**, 014440 (2007).
[13] I. N. Krivorotov *et al.*, Science **307**, 228 (2005).
[14] S. Petit *et al.*, Phys. Rev. Lett. **98**, 077203 (2007).
[15] J.-V. Kim, V. Tiberkevich, and A. N. Slavin, Phys. Rev. Lett. **100**, 017207 (2008).
[16] Z. Li and S. Zhang, Phys. Rev. B **69**, 134416 (2004).
[17] M. Gmitra and J. Barnás, Phys. Rev. Lett. **99**, 097205 (2007).
[18] H. Risken, *The Fokker-Planck Equation* (Springer-Verlag, Berlin, 1989).
[19] Q. Mistral *et al.*, Appl. Phys. Lett. **88**, 192507 (2006).